

Ferromagnetic Quantum Critical Endpoint in UCoAl

Dai AOKI^{1*}, Tristan COMBIER¹, Valentin TAUFOR¹, Tatsuma D. MATSUDA^{1,2}, Georg KNEBEL¹, Hisashi KOTEGAWA^{1,3}, and Jacques FLOUQUET¹

¹INAC, SPSMS, CEA Grenoble, 38054 Grenoble, France

²ASRC, JAEA, Tokai, Ibaraki 319-1195, Japan

³Department of Physics, Kobe University, Kobe 657-8501, Japan

Resistivity and magnetostriction measurements were performed at high magnetic fields and under pressure on UCoAl. At ambient pressure, the 1st order metamagnetic transition at $H_m \sim 0.7$ T from the paramagnetic ground state to the field-induced ferromagnetic state changes to a crossover at finite temperature $T_0 \sim 11$ K. With increasing pressure, H_m linearly increases, while T_0 decreases and is suppressed at the quantum critical endpoint (QCEP, $P_{\text{QCEP}} \sim 1.5$ GPa, $H_m \sim 7$ T). At higher pressure, the value of H_m identified as a crossover continuously increases, while a new anomaly appears above P_{QCEP} at higher field H^* in resistivity measurements. The field dependence of the effective mass (m^*) obtained by resistivity and specific heat measurements exhibits a step-like drop at H_m at ambient pressure. With increasing pressure, it gradually changes into a peak structure and a sharp enhancement of m^* is observed near the QCEP. Above P_{QCEP} , the enhancement of m^* is reduced, and a broad plateau is found between H_m and H^* . We compare our results on UCoAl with those of the ferromagnetic superconductor UGe₂ and the itinerant metamagnetic ruthenate Sr₃Ru₂O₇.

KEYWORDS: quantum critical endpoint, effective mass, metamagnetism, ferromagnetism, UCoAl, UGe₂

1. Introduction

Metamagnetism and quantum criticality in strongly correlated electron systems have attracted much interest as new quantum phases are expected. They can be related to unconventional superconductivity, non-Fermi liquid behavior and nematic phases. In the case of antiferromagnetic (or nearly antiferromagnetic) compounds, the metamagnetic transition in heavy fermion systems is well documented.^{1,2} A prototype material is CeRu₂Si₂ where a pseudo-metamagnetic transition occurs at $H_m \sim 7.8$ T and the quantum critical endpoint (QCEP) at which the 1st order metamagnetism collapses exists at negative pressure, as seen in Ce_{0.925}La_{0.075}Ru₂Si₂.^{3,4}

On the other hand, in itinerant ferromagnets, the metamagnetic transition from the paramagnetic ground state to the field-induced ferromagnetic state could occur when the system is tuned into the paramagnetic ground state at zero field. Well-known systems are the itinerant ferromagnets UGe₂,^{5,6} ZrZn₂,⁷ and the nearly ferromagnetic compound Sr₃Ru₂O₇.⁸ In particular, UGe₂ is an interesting system, because unconventional superconductivity coexisting with ferromagnetism appears near the critical pressure,⁹ and the superconducting phase is enhanced by the metamagnetic transition between two ferromagnetic phases, FM1 and FM2.¹⁰ Recently we have investigated the ferromagnetic QCEP of UGe₂ by resistivity and Hall effect measurements, and have concluded that the QCEP exists at ~ 18 T and at ~ 3.5 GPa.^{5,6} However severe experimental conditions, namely the high field, very low temperature and high pressure, prevent us from performing precise experiments above the QCEP to date. Therefore it is important to find new systems which can be easily tuned to the QCEP. In this paper, we demonstrate that UCoAl is an ideal system for this kind of study.

UCoAl crystallizes in a hexagonal structure with ZrNiAl-type (space group: $P\bar{6}2m$, No. 189) without inversion symme-

try. Applying the magnetic field along the c -axis, the paramagnetic ground state becomes a field induced ferromagnetic state through the metamagnetic transition at $H_m \sim 0.7$ T, with an induced magnetic moment $M_0 \sim 0.3 \mu_B$.¹¹ The magnetization curve is very anisotropic between $H \parallel c$ -axis and $H \perp c$ -axis, indicating Ising-like behavior. By doping with Y as a negative pressure or by applying uniaxial stress,^{12,13} ferromagnetism appears, indicating that UCoAl is in proximity to ferromagnetic order. The critical pressure where the Curie temperature T_{Curie} is suppressed to zero will be negative ($P_c \sim -0.2$ GPa)¹⁴ and the ground state at ambient pressure is already the paramagnetic one. H_m linearly increases with increasing hydrostatic pressure.¹⁴ The metamagnetic transition at H_m is identified to be of 1st order by the clear hysteresis between increasing and decreasing fields. Applying pressure, this hysteresis starts to be suppressed, which may suggest that the 1st order transition will terminate at a QCEP. However there are no experimental reports which clarify the existence of the QCEP at high pressures above 1.2 GPa. Here we report the experimental evidence for the QCEP in UCoAl detected by resistivity and magnetostriction measurements at high fields and at high pressures.

2. Experimental

Single crystals of UCoAl were grown using the Czochralski method in a tetra-arc furnace. The starting materials of U (purity: 99.95 %-3N5), Co (3N) and Al (5N) were melted on a water-cooled copper hearth under a high purity Ar atmosphere gas. The ingot was turned over and was melted again. This process was repeated several times in order to obtain a homogeneous polycrystalline ingot. The ingot was subsequently pulled with a rate of 15 mm/hr for single crystal growth. The obtained single crystal ingot was cut using a spark cutter and was oriented by X-ray Laue photograph, displaying very sharp Laue spots. The resistivity using a sample with rectan-

*E-mail address: dai.aoki@cea.fr

gular shape ($0.5 \times 0.5 \times 1 \text{ mm}^3$, c -axis long) was measured by a four probe AC method ($f \sim 17 \text{ Hz}$) for the electrical current along $[10\bar{1}0]$ direction ($J \perp c$ -axis) at low temperatures down to 0.1 K and at high fields up to 16 T for the field along $[0001]$ direction ($H \parallel c$ -axis). The residual resistivity ratio (RRR) was approximately 10. The magnetostriction was measured using strain gauges by the active dummy method with a wheatstone bridge at temperatures down to 2 K using a lock-in amplifier ($f \sim 17 \text{ Hz}$). The gauge was glued on the surface of the sample with the dimension of $2 \times 2 \times 0.4 \text{ mm}^3$, so that it detects the dilatation along the c -axis (ΔL_c). Both resistivity and magnetostriction measurements were performed under pressure up to 2.4 GPa using a CuBe-NiCrAl hybrid type piston cylinder cell with Daphne oil 7373 as a pressure medium. The pressure was determined by the superconducting transition temperature of Pb. The sharp transition assures that the pressure gradient is small ($< 0.05 \text{ GPa}$) for all pressure range. However, the pressure gradient for magnetostriction measurements with a relatively large sample is larger, which is approximately 0.1 GPa in maximum.¹⁵⁾ The Daphne oil 7373 solidifies at 2.2 GPa at room temperature,¹⁶⁾ thus the hydrostaticity is good at least up to $\sim 2 \text{ GPa}$ at low temperatures. For comparison with the field dependence of the resistivity A coefficient, the specific heat was measured by the relaxation method at ambient pressure under magnetic field up to 9 T and at low temperature down to 0.45 K. Angular dependences of H_m from $H \parallel c$ -axis to $H \perp c$ -axis ($H \parallel [10\bar{1}0]$) were also measured at ambient pressure by magnetization and magnetostriction. The magnetization was measured at temperatures down to 2 K and at magnetic fields up to 5.5 T using a SQUID magnetometer. The magnetostriction was measured employing the same manner as under pressure at temperatures down to 2 K and at fields up to 9 T using a horizontal-axis sample rotator.

3. Experimental results

3.1 Ambient pressure and angular dependence

Figure 1 show the susceptibility and magnetization at 2 K. A very anisotropic susceptibility response is found between $H \parallel c$ and $H \perp c$ -axis, indicating the Ising-type behavior, which is in good agreement with the previous results.^{17–19)} For $H \parallel c$ -axis, the susceptibility shows a broad maximum around 20 K, while no anomaly is observed for $H \perp c$ -axis. This behavior is typical for heavy fermion systems, such as CeRu_2Si_2 , UPt_3 , URu_2Si_2 . Applying the magnetic field along c -axis at low temperature, a sharp metamagnetic 1st order transition is observed at $H_m \sim 0.7 \text{ T}$, with a hysteresis between the up-sweep and down-sweep measurements.

First we focus on the angular dependence of the metamagnetic transition, since in the well-known ferromagnetic systems, such as URhGe ,^{20–23)} UCoGe ^{24–26)} and $\text{Sr}_3\text{Ru}_2\text{O}_7$ (nearly ferromagnetic compound),²⁷⁾ the field angle is found to be a tuning parameter for the quantum singularities, as pressure is. By increasing the field angle θ from $H \parallel c$ -axis to $H \perp c$ -axis, H_m shifts to higher fields proportional to $1/\cos\theta$. It should be noted that the induced moment just above H_m decreases with θ , which roughly follows $\cos\theta$ dependence. This is different from the pressure response of magnetization up to 1.2 GPa for $H \parallel c$ -axis, where the induced moment just above H_m remains almost at the same value, $\sim 0.3 \mu_B$, while H_m is

monotonously increased with pressure.¹⁴⁾ The field angle response is obviously different from the pressure response in UCoAl.

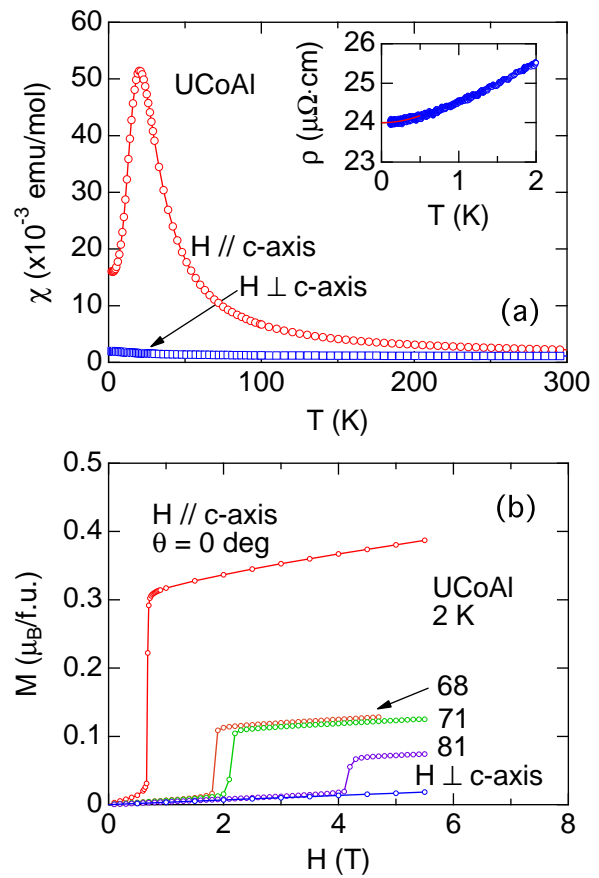


Fig. 1. (Color online) (a) Temperature dependence of the susceptibility at 1 kOe for $H \parallel c$ -axis and $H \perp c$ -axis in UCoAl. (b) Magnetization curves with increasing field at 2 K at different field angles θ from $H \parallel c$ -axis to $H \perp c$ -axis. The inset of panel (a) shows the temperature dependence of resistivity at zero field, indicating that T^2 dependence is preserved at least up to 0.5 K within experimental precision.

Figure 2(a) show the field dependence of the magnetostriction $\Delta L_c/L_c$ for different field angles at 2 K. Sharp drops of magnetostriction due to the metamagnetic transition in agreement with the previous results²⁸⁾ are observed at H_m , which is increased with increasing field angle. As shown in Fig. 2(b), H_m increases following a $1/\cos\theta$ dependence, at least up to 7.2 T at 84 deg. The magnitude of the jump of magnetostriction retains a large value even at high field angles. Furthermore the hysteresis at H_m , ΔH_{hyst} also increases with field angle, following the $1/\cos\theta$ dependence, as shown in the inset of Fig. 2(b). It is noted that the width of metamagnetic transition ($\Delta H_m \sim 0.02 \text{ T}$) shows no significant increase with field angle, indicating that the sharp metamagnetic transition is retained up to 84 deg. These results indicate that the 1st order nature is very robust against the field angle, which cannot be a tuning parameter to a QCEP in UCoAl at least at ambient pressure.

It should be noted that Fermi liquid properties are observed in the resistivity measurements, as shown in the inset

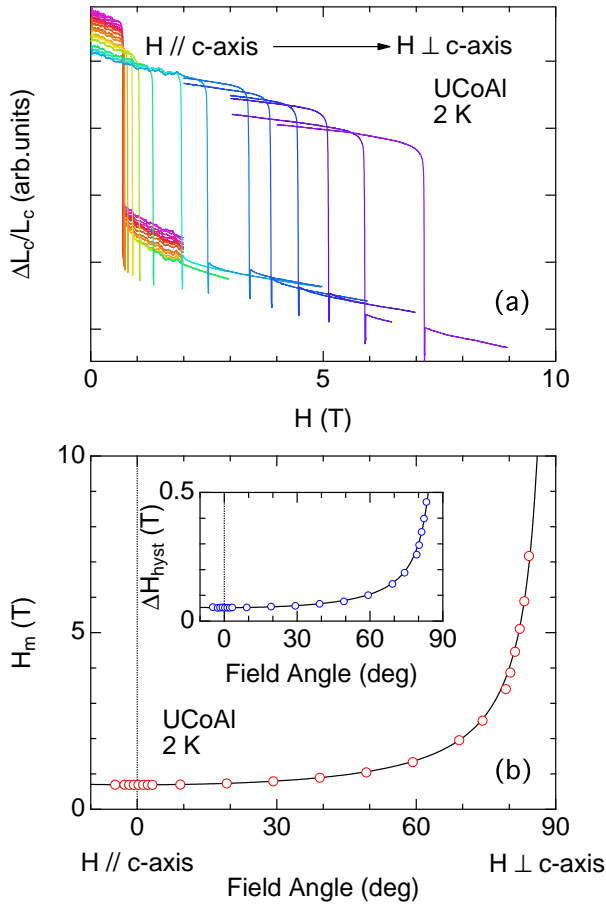


Fig. 2. (Color online) (a) Field dependences of the magnetostriction with increasing fields at 2 K at different field angles from $H \parallel c$ -axis to $H \perp c$ -axis in UCoAl. (b) Angular dependence of the metamagnetic transition field H_m at 2 K for up-sweep measurements. The inset of panel (b) shows the angular dependence of the hysteresis of H_m between up-sweep and down-sweep. The solid lines correspond to a $1/\cos \theta$ dependence.

of Fig. 1(a), where the resistivity follows the T^2 dependence below 0.5 K, in good agreement with very low temperature specific heat data.¹⁸⁾ Thus, the achievement of a very low temperature ($T < 0.5$ K) is a necessary condition to observe the Fermi liquid regime at ambient pressure.

3.2 Pressure study

Figure 3(a) shows the field dependence of the magnetoresistance at ambient pressure for different constant temperatures. Anomalies due to the metamagnetic transition from the paramagnetic state to the field-induced ferromagnetic state are clearly observed around $H_m \sim 0.7$ T. The anomaly with a small step-like decrease at low temperatures gradually changes into a sharp peak around 10 K. Further increasing temperature, the anomaly is smeared out. Figure 3(b) shows the temperature variation of H_m . H_m slightly shifts to higher fields with increasing temperature implying that the ferromagnetic correlations play a main role for the metamagnetism in UCoAl, as observed just above P_c in UGe₂.⁵⁾ At low temperatures, H_m is obviously identified as the 1st order transition, since hysteresis between the up-sweep- and the down-sweep-field is observed in magnetoresistance. With increasing tem-

perature, H_m changes from 1st order to a crossover at T_0 . Here we determined T_0 from the field derivative of magnetoresistance, $d\rho/dH$. As shown in the inset of Fig. 3(b), $d\rho/dH$ reveals sharp maximum and minimum below and above H_m . When the peak-to-peak amplitude of $d\rho/dH$ becomes maximum, meaning an acute peak of the magnetoresistance, we define this temperature as T_0 . In Fig. 3, T_0 is found to be 11 K. This value is in good agreement with that obtained from the hysteresis of H_m in the magnetostriction measurements, as mentioned later, supporting the validity of our definition for T_0 .

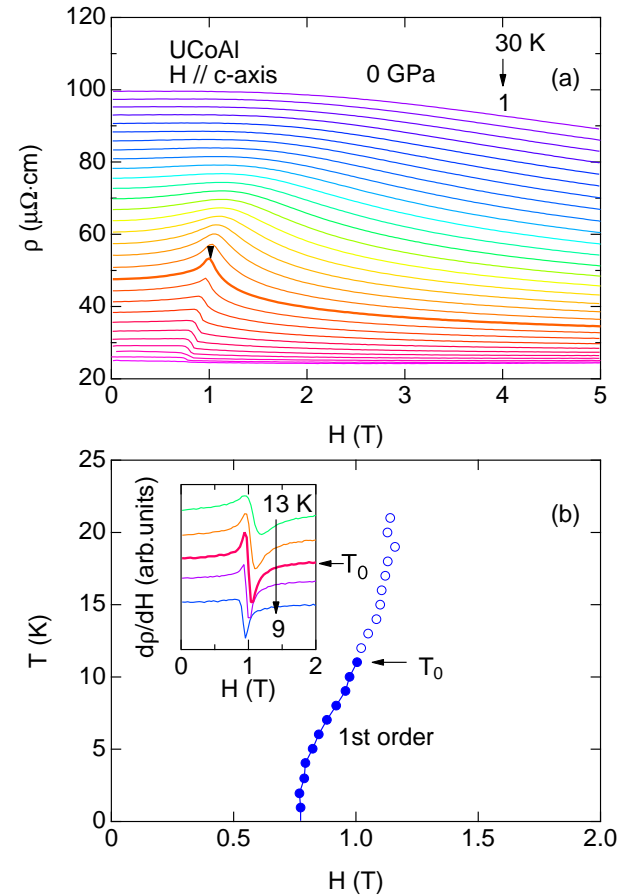


Fig. 3. (Color online) (a) Magnetoresistance with increasing fields for $H \parallel c$ -axis at various constant temperatures from 1 to 30 K with 1 K step in UCoAl. (b) Temperature variation of the metamagnetic transition field H_m . The inset shows the field derivative of magnetoresistance. The thick line corresponds to data at $T_0 = 11$ K, at which the metamagnetic transition changes from the 1st order to the crossover.

Figure 4(a) shows the field dependence of the magnetostriction at ambient pressure for different constant temperatures. Sharp drops of the magnetostriction are observed at H_m at low temperatures. This is in good agreement with the previous report.²⁸⁾ At high temperatures, the anomalies at H_m become broad and finally they are smeared out. As shown in the inset of Fig. 4(c), a hysteresis ($\Delta H_{\text{hyst}} \sim 0.06$ T) is clearly observed at 2 K between up and down field sweeps indicating the 1st order transition at low temperatures. ΔH_{hyst} decreases with increasing temperatures and finally becomes zero

at $T_0 \sim 11$ K, which is in good agreement with the value obtained by the magnetoresistance measurements as shown in Fig. 3. The transition at H_m changes to a crossover above T_0 .

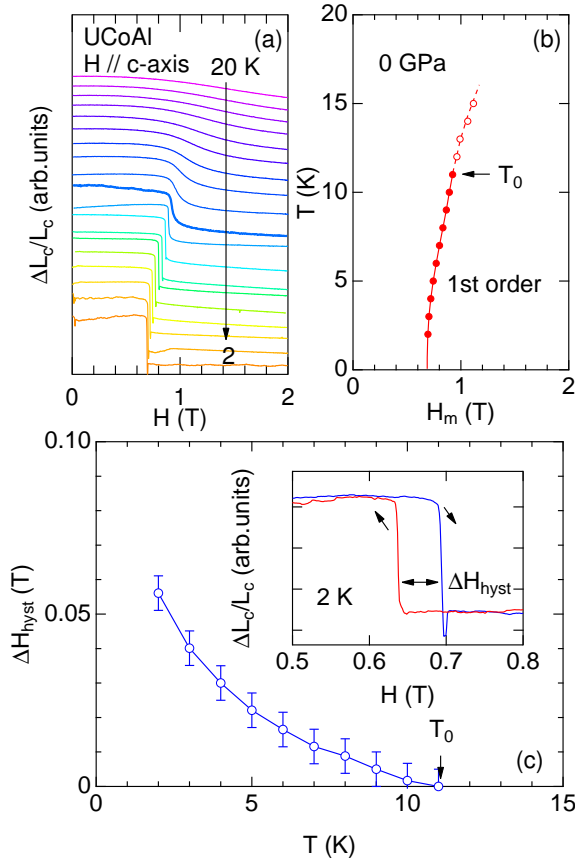


Fig. 4. (Color online) (a) Field dependence of the magnetostriction along c -axis for $H \parallel c$ -axis at various constant temperatures from 20 to 2 K with 1 K. (b) Temperature evolution of the metamagnetic transition field H_m . The inset of panel (c) displays the hysteresis of H_m at 2 K between increasing and decreasing field. (c) Temperature dependence of the hysteresis field ΔH_m .

As shown in Fig. 5, the hysteresis is suppressed by applying pressure. With increasing pressure, ΔH_{hyst} at 2 K is markedly suppressed from 0.06 T at ambient pressure to ~ 0.015 T at 1.31 GPa. No hysteresis was observed at higher pressures ($P \geq 1.75$ GPa). Correspondingly, T_0 decreases with pressures. It is, however, difficult to evaluate the value of T_0 precisely for different pressures, because T_0 is too small for the magnetostriction measurements using strain gauges, giving rise to relatively large error bars of ΔH_{hyst} . Nevertheless, the present results imply that the 1st order transition at H_m will terminate at high pressure probably above $P_{\text{QCEP}} \sim 1.5$ GPa.

Figure 6(a) shows the field dependence of the magnetostrictions at 2 K at various pressures. Increasing pressure, H_m increases linearly to high fields and reaches 11 T at 2.4 GPa. Here we define H_m from a midpoint of the magnetostriction jump. The amplitude of the jump ($\equiv \delta L$) decreases with pressure and most likely remains constant above $P_{\text{QCEP}} \sim 1.5$ GPa, as shown in Fig. 6(b). On the other hand, the transition width ($\equiv \Delta H_m$) is almost constant or slightly increases

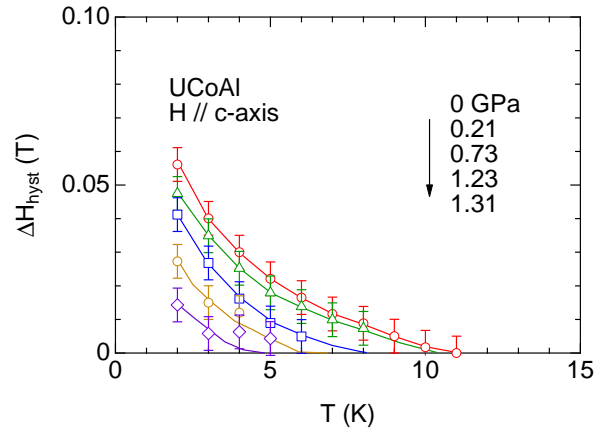


Fig. 5. (Color online) Temperature dependence of the hysteresis field ΔH at various pressures in UCoAl.

up to 1.5 GPa, and then rapidly increases with further increasing pressure, as shown in Fig. 6(c). One can speculate that the quantum critical endpoint (QCEP) is located around $P_{\text{QCEP}} \sim 1.5$ GPa. At first approximation, the magnetic contribution of the magnetovolume effect $\Delta V_m/V_m$ is related to the magnetization M via the relation, $\Delta V_m/V_m \propto M^2$. According to the previous magnetization measurements under pressure up to 1.2 GPa,¹⁴⁾ the initial slope of magnetization is unchanged, but H_m increases with pressure, while the induced moment above H_m is constant ($\sim 0.3 \mu_B$). The present results in Fig. 6 should be related to the pressure response of magnetization curve.

Figure 7 shows the magnetoresistance at different constant temperatures at two different pressures below and above P_{QCEP} . At 1.23 GPa ($< P_{\text{QCEP}}$), the magnetoresistance shows the very sharp peak at $H_m = 5.7$ T at 1.9 K, which is quite different from that at ambient pressure where the step-like behavior is observed at low temperatures. From the analysis of $d\rho/dH$ as in the inset of Fig. 3(b), T_0 at 1.23 GPa is found to be 4 K, which is reduced from the original value, $T_0 = 11$ K at ambient pressure.

On the other hand, at 2.36 GPa ($> P_{\text{QCEP}}$), the magnetoresistance shows a plateau around H_m at low temperatures. Two kinks are observed at $H_m = 10.5$ T and $H^* = 12$ T at the lowest temperature. The former kink at 10.5 T is fairly in good agreement with the results of magnetostriction as shown in Fig. 6(a). However, the latter kink at 12 T was only observed in the magnetoresistance measurements, while no anomaly was detected at 12 T in the magnetostriction measurements. Two kinks are merged and broadened at high temperatures. Interestingly, another broad hump is observed around 5 T only at low temperatures.

From the temperature dependence of the resistivity at constant field, we determined the field dependence of the resistivity A coefficient and the residual resistivity ρ_0 at different pressures, as shown in Fig. 8(b)(c). Here the resistivity is described by $\rho = \rho_0 + AT^2$. Considering the Kadowaki-Woods relation ($A \propto \gamma^2$, γ : Sommerfeld coefficient) based on the existence of the strong local fluctuation, the field dependence of the A coefficient corresponds to that of the square of the effective mass m^* ($A \propto \gamma^2 \propto m^{*2}$). For comparison, the field depen-

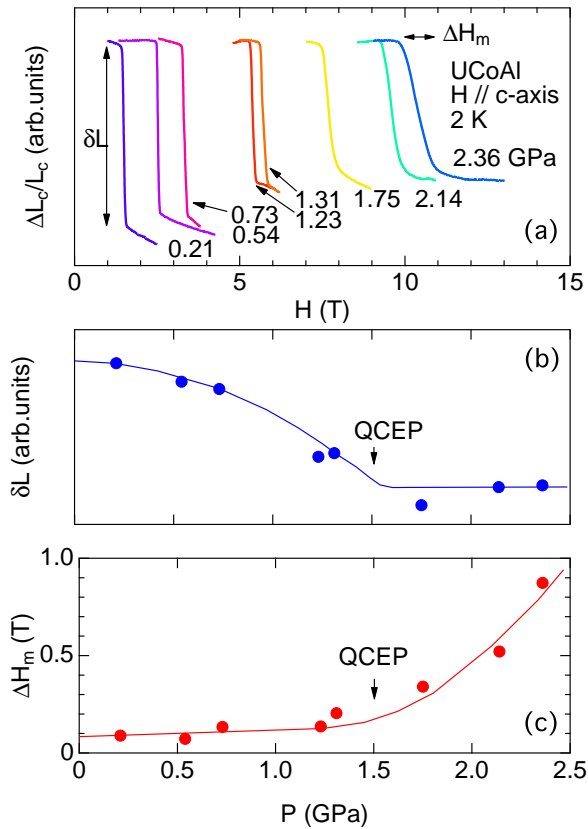


Fig. 6. (Color online) (a) Field dependence of the magnetostrictions for $H \parallel c$ -axis at various pressures at 2 K in UCoAl. (b) Pressure dependence of the amplitude of jumps in magnetostriction at H_m . (c) Pressure dependence of the transition width. QCEP is located around 1.5 GPa.

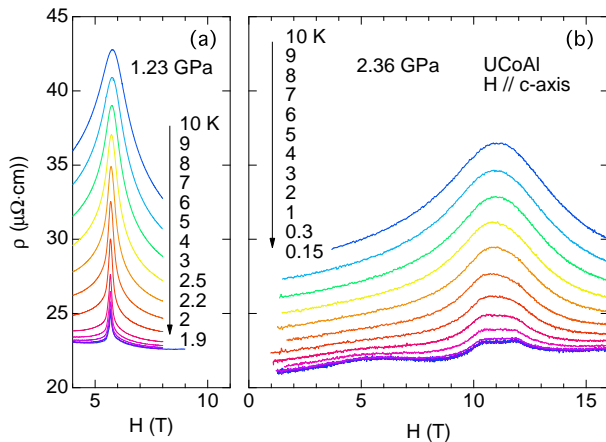


Fig. 7. (Color online) Field dependence of the magnetoresistance at various fixed temperatures at two different pressures, 1.23 GPa ($< P_{\text{QCEP}}$) and 2.36 GPa ($> P_{\text{QCEP}}$) for $H \parallel c$ -axis in UCoAl.

dependence of the γ -value at ambient pressure estimated from the measurements at 0.45 K is also shown in Fig. 8(a). The results are consistent with the previous results¹⁸⁾ The γ -value at zero field is 75 mJ/K²mol, which is almost unchanged up to H_m . Further increasing field, the γ -value is abruptly reduced down to 60 mJ/K²mol and is almost constant up to 9 T. It should be

noted that the slight upturn at high fields is due to the hyperfine contribution from Co and Al. This is roughly consistent with the field dependence of A coefficient at ambient pressure shown in Fig. 8(a). However, the normalization to the high field limit will lead to an enhancement of \sqrt{A} at zero field in agreement with the enhancement of \sqrt{A} with respect to γ in ferromagnetic spin fluctuation theory.

With increasing pressure, the field dependence of the A coefficient is drastically changed, as shown in Fig. 8(b). H_m increases linearly with field, and the A coefficient at zero field is suppressed with pressure. Instead, the peak structure at H_m becomes pronounced. At 1.23 GPa, the A coefficient reveals a very sharp peak at H_m , which is approximately three times larger than that at zero field. Further increasing pressure, the peak value of A coefficient is reduced and the width of the peak is significantly increased. Above $P_{\text{QCEP}} \sim 1.5$ GPa, the A coefficient exhibits a plateau.

In order to see the pressure evolution of the A coefficient more clearly, we plot the pressure dependence of the A coefficient at H_m and at zero field, as shown in Fig. 9. The A coefficient at zero field, $A(0)$, monotonously decreases in Fig. 9(b), indicating that the pressure drives UCoAl away from the critical region. On the other hand, the A coefficient at H_m , $A(H_m)$, shows a maximum around the QCEP. If we take the ratio, $A(H_m)/A(0)$, the enhancement of $A(H_m)$ at QCEP is more significant, as shown in Fig. 9(c). It is interesting to note that the value of $A(H_m)/A(0)$ seems to remain constant above P_{QCEP} .

The residual resistivity shows a plateau, as well (see Fig. 8(c)). The kink of the plateau at lower field, for example, $H_m = 10.5$ T at 2.36 GPa corresponds to the continuation of H_m , which was detected by the magnetostriction (see Fig. 6(a)). However, the kink of the plateau at higher field (ex. $H^* = 12$ T at 2.36 GPa) was detected only by the resistivity, but the magnetostriction down to 0.3 K shows no anomaly. Interestingly, the residual resistivity exhibits a sharp peak around P_{QCEP} . This is in good agreement with the prediction of residual resistivity enhancement at the ferromagnetic singularity.²⁹⁾ Furthermore, a broad anomaly is observed around 6 T at 2.36 GPa, which shifts to lower field with decreasing pressure. These broad anomalies might be explained by the competitive phenomena between the scattering near H_m and the orbital effect of transverse magnetoresistance, which is related to the value of $\omega_c\tau$ where $\omega_c (= eH/m^*c)$ and τ are the cyclotron frequency and the scattering lifetime, respectively.

It should be noted that temperature range where the resistivity follows a T^2 relation becomes narrower around QCEP, as shown in Fig. 10. For example, at 1.56 GPa, T^2 behavior was observed only up to ~ 1 K at 7.3 T. An interesting point is to investigate the critical exponent of resistivity at the QCEP, which is left for future studies of precise resistivity measurements.

Figure 11 shows the pressure dependence of H_m extrapolated to 0 K obtained by the magnetoresistance and magnetostriction measurements. H_m is almost linearly increased with pressure up to 7 T at $P_{\text{QCEP}} \sim 1.5$ GPa. The value of H_m from the resistivity measurements almost coincides with that from the magnetostriction measurements, although H_m of resistivity is slightly higher than that of magnetostriction, which is most likely due to the slight pressure inhomogeneity in the pressure cell. Above P_{QCEP} , the magnetostriction shows

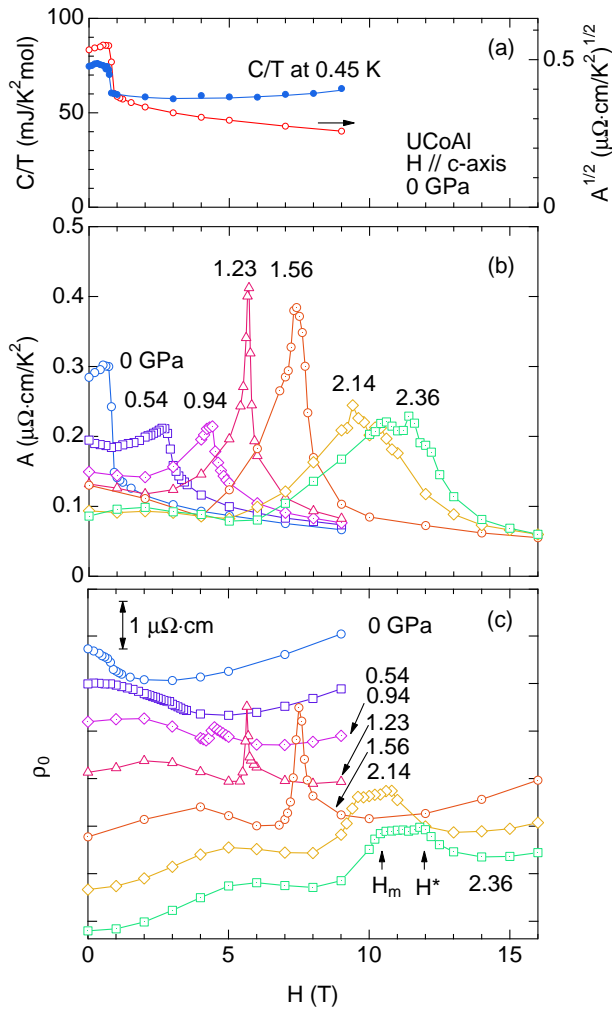


Fig. 8. (Color online) (a) Field dependence of the specific heat at 0.45 K for $H \parallel c$ -axis in UCoAl. (b) Field dependence of the resistivity A coefficient at various pressures and (c) corresponding residual resistivity. The data in panel (c) is vertically shifted for clarity. In panel (a), the field dependence of A coefficient is plotted, as well, in the form of \sqrt{A} vs H , assuming Kadowaki-Woods relation.

the linear increase of H_m continuously, while the magnetoresistance shows the split corresponding to the plateau of the residual resistivity. The lower field anomaly is in good agreement with the results of magnetostriction.

Figure 11(b) shows the pressure dependence of T_0 at which the 1st order transition of H_m terminates and changes into a crossover. The value was evaluated by the field derivative of magnetoresistance, as shown in the inset of Fig. 3(b). T_0 decreases with pressure, and collapses around $P_{\text{QCEP}} \sim 1.5$ GPa, indicating that the 1st order transition at H_m terminates at P_{QCEP} , and a new phase appears above P_{QCEP} .

As a summary of pressure experiments, we schematically show in Fig. 12 the temperature–pressure–field phase diagram of UCoAl, together with the field–pressure phase diagram at 0 K. The critical point where T_{Curie} is suppressed to 0 K is at a negative pressure ($P_c \sim -0.2$ GPa) in UCoAl. At the tricritical point (TCP), T_{Curie} bifurcates and the 1st order plane appears. When the magnetic field is applied at ambient pressure, UCoAl crosses the 1st order plane, which corresponds to the metamagnetic transition from paramagnetic

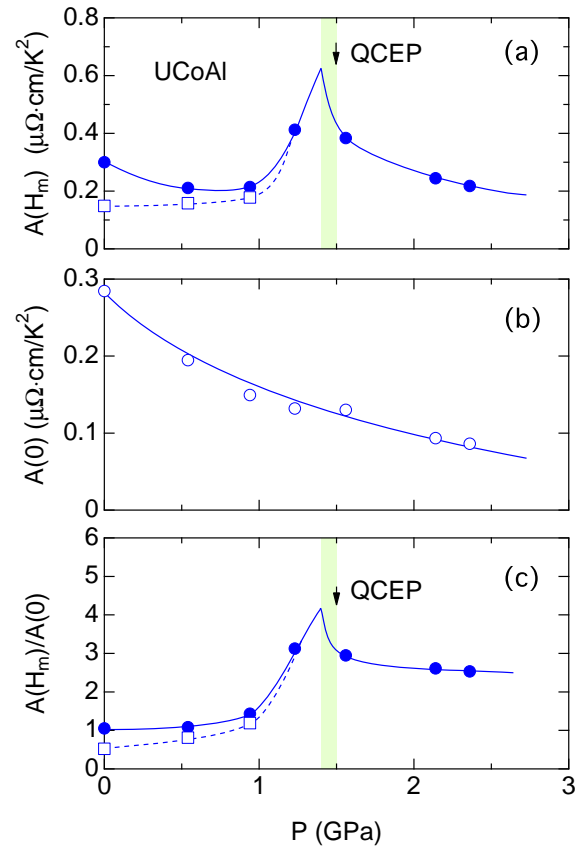


Fig. 9. (Color online) Pressure dependence of the A coefficient (a) at H_m and (b) at zero field in UCoAl. (c) Pressure dependence of the ratio of $A(H_m)$ to $A(0)$. Closed symbols and open symbols in panel (a) and (c) correspond to the peak value and dropped value at H_m , respectively. The lines are guides to the eyes.

ground state to the field-induced ferromagnetic state. The temperature, which is located on the 1st order plane at finite temperature, corresponds to T_0 . Increasing pressure, H_m increases linearly and meets with QCEP where T_0 is suppressed to 0 K. At QCEP, the effective mass shows the acute enhancement. At higher pressure $P > P_{\text{QCEP}}$, H_m increases continuously as a crossover, which can be observed both by resistivity and by magnetostriction. From the QCEP, a new transition or crossover line at H^* which was detected in ρ_0 appears and deviates from the original H_m line.

4. Discussion

A general treatment³¹⁾ implies that the ferromagnetic phase diagram with a strong decrease of T_{Curie} near P_c will be extended in magnetic field by a first order line T_0 which will terminate at a pressure higher than P_c . In a conventional approach, the paramagnetic–ferromagnetic transition at H_m has been described with special features in the density of states such as a double peak structure or van Hove singularity.^{32–34)} It has also been treated in spin fluctuation theory assuming Fermi surface invariance through H_m or quite generally by considering excitations at the Fermi level which introduce non-analytic corrections in the Landau expression of the free energy^{30,35,36)} It was, however, recently stressed that a strong modification of the Fermi surface can occur at H_m . A recent

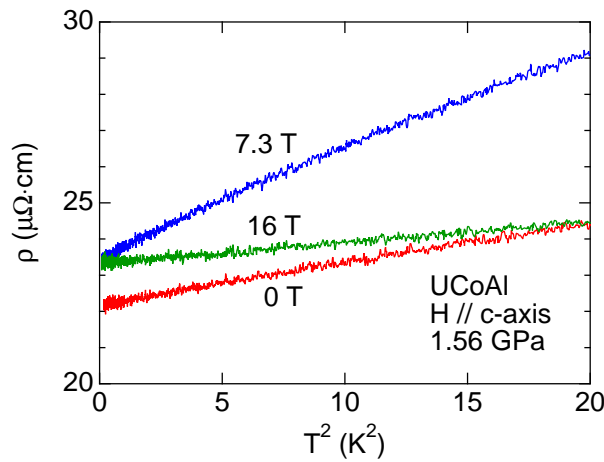


Fig. 10. (Color online) Temperature dependence of the resistivity at 0, 7.3 ($\sim H_m$) and 16 T for $H \parallel c$ -axis under pressure at 1.56 GPa in UCoAl.

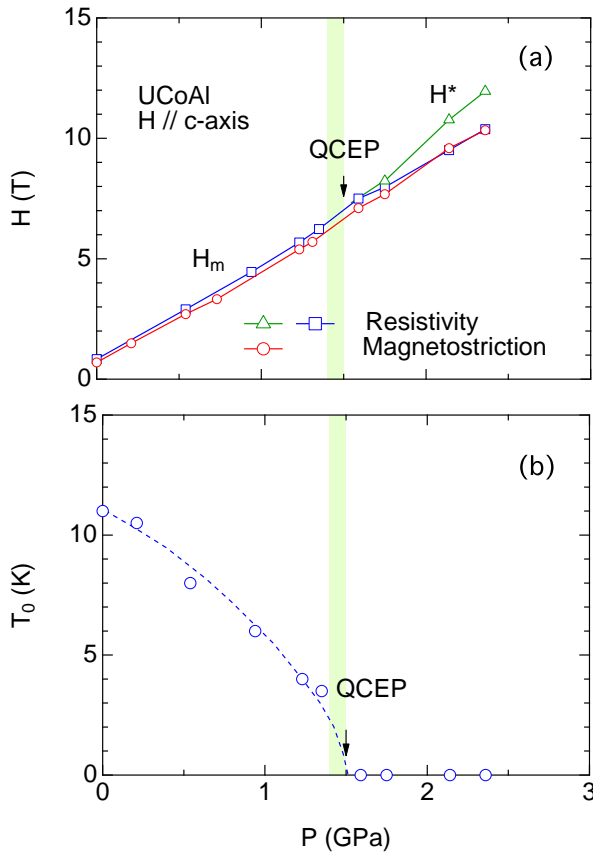


Fig. 11. (Color online) (a) Pressure dependence of H_m extrapolated to 0 K for $H \parallel c$ -axis in UCoAl, and (b) the pressure dependence of T_0 where the 1st order transition changes into the crossover.

calculation assuming that a Lifshitz transition may occur at H_m shows that the ferromagnetic wing structure on the phase diagram will be strongly affected in this case.³⁷⁾

Here we compare the present results of UCoAl with those recently obtained for the other Ising ferromagnet UGe₂. At ambient pressure, UGe₂ has a high Curie temperature $T_{\text{Curie}} \sim 52$ K associated with a large ferromagnetic ordered moment

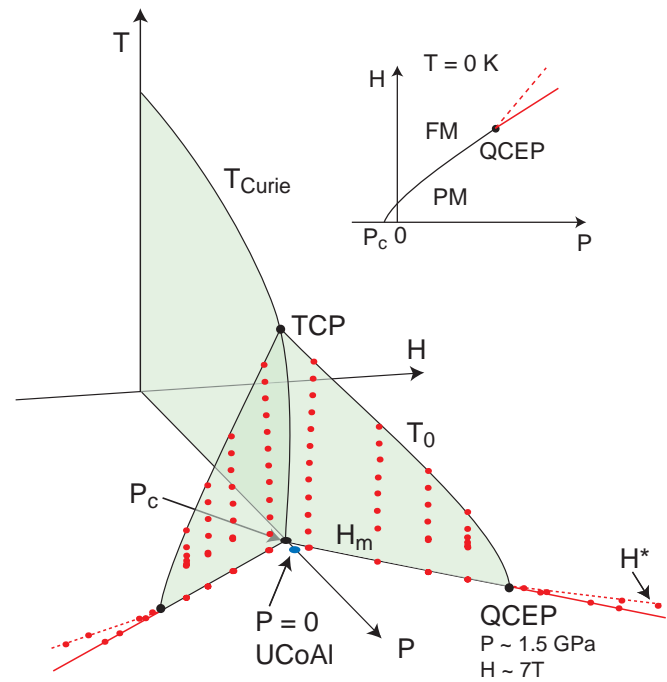


Fig. 12. (Color online) Semi-schematic temperature-pressure-field phase diagram. Red closed circles correspond to the experimental data points. The Curie temperature T_{Curie} is suppressed with pressure and bifurcates at the tricritical point (TCP), where the transition changes from 2nd order to 1st order, revealing the 1st order plane. The boundary between the 1st order and the crossover at finite temperature is called T_0 . UCoAl at ambient pressure is located just above the critical pressure P_c at which T_{Curie} collapses at $H = 0$. Applying magnetic fields, the metamagnetic transition occurs at H_m crossing the 1st order plane. Increasing pressure, H_m increases, while T_0 decreases and terminate at the quantum critical endpoint (QCEP). Above P_{QCEP} H_m continuously increases. From QCEP, new anomaly appears, as indicated by the dashed line. It is noted that the data points at “negative” fields are depicted as a mirror of those at “positive” field for the comparison with a generic phase diagram near FM instabilities.³⁰⁾

$M_0 \sim 1.5 \mu_B$. The tricritical point (TCP) is located at $T_{\text{TCP}} \sim 24$ K and $P_{\text{TCP}} \sim 1.42$ GPa. The ferromagnetism disappears at $P_c \sim 1.5$ GPa at zero field via a sharp drop of the magnetization $\Delta M_0 \sim 0.9 \mu_B$ with a 1st order nature.³⁸⁾ Due to the large value of ΔM_0 in UGe₂, the QCEP is achieved at high pressure ($P_{\text{QCEP}} \sim 3.5$ GPa $\sim 2P_c$) and high field ($H_{\text{QCEP}} \sim 18$ T).

Figure 13 shows the pressure dependence of T_0 as a function of the scaled pressure, $(P - P_c)/(P_{\text{QCEP}} - P_c)$ in UCoAl and UGe₂.⁶⁾ In UGe₂, T_0 has an upward (concave) curvature, while in UCoAl T_0 shows a downward (convex) curvature. This difference might correspond to a difference of Fermi surface dimensionality between the two compounds. In the ferromagnetic state of UGe₂, both dHvA experiments^{39–44)} and band structure calculation^{45,46)} show a quasi-two dimensional Fermi surface at least for a main dHvA branch. Such lower dimensionality can explain the upward curvature of T_0 .³⁵⁾ Up to now, there are no reports concerning Fermi surface topology on UCoAl, although band structure calculations have been reported.^{47,48)} However, three dimensionality is expected from the crystal structure. It should be noted that the crystal structure without inversion symmetry in UCoAl may also affect the pressure response of T_0 .

The difference between the two compounds is confirmed by the field dependence of the resistivity A coefficient, as

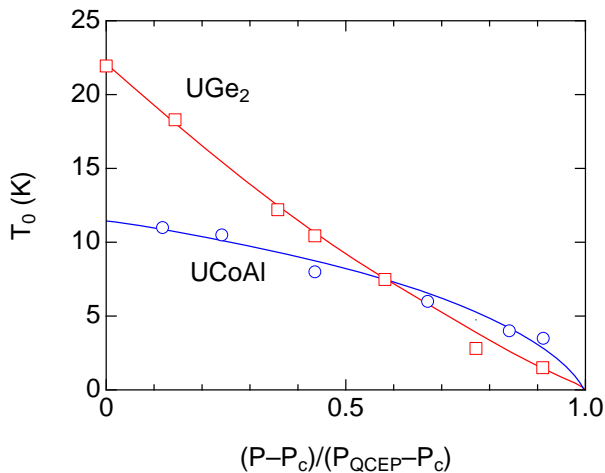


Fig. 13. (Color online) Scaled pressure dependence of T_0 of UCoAl and UGe₂. In UCoAl, the critical pressure P_c and the pressure at QCEP are -0.2 GPa and 1.5 GPa, respectively. In UGe₂, P_c and P_{QCEP} are 1.5 GPa and 3.6 GPa, respectively. The data of UGe₂ are cited from ref.6.

shown in Fig. 14. In UGe₂, the A coefficient shows a step-like increase at H_m at pressures just above P_c ($P = 1.8$ GPa $> P_c$),⁶⁾ as shown in Fig.14(a), while the A coefficient near P_c in UCoAl shows a step-like decrease at H_m . However, near P_{QCEP} , the field dependence of the A coefficient for both UCoAl and UGe₂ shows a similar peak structure at H_m , where the enhanced values for both compounds are three times larger than those at zero field, although the peak of UCoAl is much sharper than that of UGe₂. This observation is consistent with the effect of lower dimensionality in UGe₂. It is indeed predicted as $A \sim (|H - H_{QCEP}|/H_{QCEP})^{-1/3}$ for $d = 3$ (3D system) and $A \sim (|H - H_{QCEP}|/H_{QCEP})^{-2/3}$ for $d = 2$ (2D system),³⁵⁾ as shown in the inset of Fig. 14(c) but for both cases, the data cannot be fully fitted with a spin fluctuation approach. A possible reason might be unusual critical exponent around H_{QCEP} . The present results of A coefficient are obtained, assuming that the resistivity follows T^2 at low temperatures just above 0.1 K. More precise measurements at lower temperatures is left for the future study. That will allow a definitive comparison with a spin fluctuation approach.

The difficult question is possible changes of the Fermi surface at H_m . In UGe₂, the drastic change of the Fermi surface between the paramagnetic state and the ferromagnetic state (FM1) was directly observed by de Haas-van Alphen (dHvA) experiments.⁴⁰⁻⁴⁴⁾ Nevertheless, it is still an open question whether the Fermi surface changes near the QCEP because of the large values of P_{QCEP} and H_{QCEP} . The change of Fermi surface associated with a Lifshitz transition near P_{QCEP} might be a possible origin for the deviation of T_0 and A from the spin fluctuation theory.

Up to now, no clear quantum oscillation experiments has been reported for UCoAl. However, the Hall coefficient and thermopower coefficient at ambient pressure reveal a drastic change through H_m ,⁴⁹⁾ also suggesting a change of Fermi surface. An interesting point in UCoAl is that the measurements can be easily achieved far above P_{QCEP} .

A new feature in the present study is that further increasing pressure above QCEP, the transition line continues as a

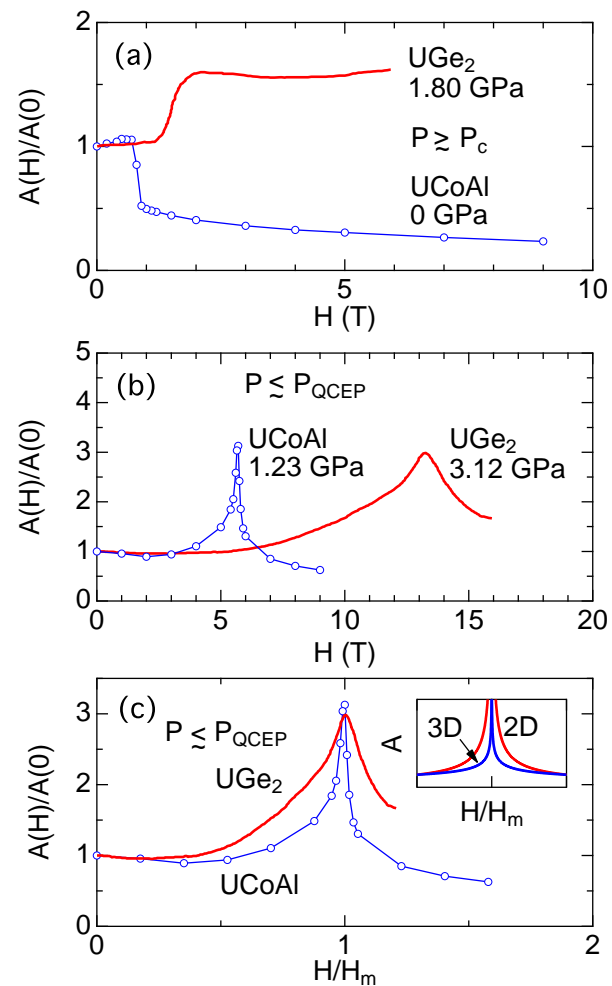


Fig. 14. (Color online) Field dependence of the A coefficient (a) just above P_c and (b) just below P_{QCEP} in UCoAl and UGe₂. A coefficient is normalized with the value of zero field. (c) Field is normalized with H_m from panel (b). The inset of panel (c) shows the prediction from the spin fluctuation theory for two and three dimensional cases. The data of UGe₂ are cited from ref.6.

crossover line from the 1st order metamagnetic transition and a new high field phase appears. Theoretically, a new mechanism caused by the topological change of Fermi surface related to the Lifshitz-type transition is proposed at QCEP, where the unusual behavior ($d\chi^{-1}/dM \rightarrow \infty$, χ : susceptibility, M : magnetization) is predicted.^{37,50)}

Another interesting result is that the field dependence of ρ_0 appears to have a plateau for $P > P_{QCEP}$ associated with a plateau in the field dependence of A . For example at 2.36 GPa, the plateau extends from 10 to 12 T. It should be noted that the present experimental setup means transverse magnetoresistance, which can be affected by the orbital effect of the cyclotron motion, namely $\omega_c\tau$ ($\omega_c = eH/m_c^*$). If the orbit is associated with van Hove singularity and a Lifshitz transition, a feedback can occur on the variation of the cyclotron effective mass m_c^* .

In general, a field sweep on a system with a sharp singularity in the density of states can lead to a large variety of phenomena: collapse or change of interactions (balance

between ferromagnetic and antiferromagnetic channel), field dependence of local fluctuations (Kondo effect and valence fluctuations)^{1,51)} and field evolution of Fermi surfaces (Lifshitz transition and/or Pauli depairing of small Fermi surface sheets).^{52–54)} A recent appealing possibility will be the occurrence of nematic phase as suggested in $\text{Sr}_3\text{Ru}_2\text{O}_7$ ^{55,56)}

A simple way to understand the plateau is to assume two different contributions; one is located at H_m and the other is located at H^* . For example, through the studies of metamagnetic phenomena in CeRu_2Si_2 family, a plateau of the field dependence of effective mass is detected in $\text{Ce}(\text{Ru}_{0.92}\text{Rh}_{0.08})_2\text{Si}_2$ between $H_c = 3\text{ T}$ and $H_m = 5.5\text{ T}$.⁵⁷⁾ The details will be published elsewhere. In the pure system CeRu_2Si_2 , it is known that two singularities attributed to antiferromagnetic fluctuations and the ferromagnetic fluctuations occur at the same field $H_m \sim 7\text{ T}$,⁴⁾ as detected by neutron scattering experiments.⁵⁸⁾ However, in $\text{Ce}(\text{Ru}_{0.92}\text{Rh}_{0.08})_2\text{Si}_2$, two singularities might be separated. Although the microscopic experimental evidence is not yet obtained, the simple image is that the nature of antiferromagnetic order is strongly modified by Rh-doping going from the transverse (La-doping) to longitudinal antiferromagnetic mode at zero field. However, the fact that the magnetic field favors the transverse mode in antiferromagnetic correlations leads to a switch in the paramagnetic phase with only strong antiferromagnetic correlations at H_c ; the subsequent crossing through a regime dominated by ferromagnetic fluctuations occurs at H_m which is higher than H_c . In UCoAl , similar two contributions may give rise to the plateau of effective mass.

The plateau observed in UCoAl above P_{QCEP} has some similarities with the results of $\text{Sr}_3\text{Ru}_2\text{O}_7$, which are interpreted as a signature of a nematic fluid which is characterized as a translationally invariant metallic phase with a spontaneously generated spatial anisotropy.⁵⁶⁾ This proposal supports the idea that strongly correlated electrons can self-organize in quite different fashions and the metamagnetism here is not the only possibility. The possibility of a nematic phase in $\text{Sr}_3\text{Ru}_2\text{O}_7$ has been mainly given by the field-angle tuned magnetoresistance and the anisotropy.⁵⁵⁾ Recent pressure experiments have clearly shown that the uniform magnetization density is not the order parameter near QCEP but clear signatures of nematic phase were not observed.⁵⁹⁾ It is worthwhile to remark that UCoAl is a Ising 3D system with respect to the Fermi surface properties, while $\text{Sr}_3\text{Ru}_2\text{O}_7$ is a Heisenberg type with 2D Fermi surfaces. As shown in Figs. 1 and 2, UCoAl has strong Ising nature where H_m strongly increases with a $1/\cos\theta$ dependence, while H_m in $\text{Sr}_3\text{Ru}_2\text{O}_7$ shows the moderate increase from 5 T for $H \parallel ab$ -plane to $\sim 7.8\text{ T}$ for $H \parallel c$ -axis. Basically, in UCoAl at least at low pressures, the key ingredient is the component of the magnetization along the c -axis. There is no relation between field-angle and pressure for singularities. An interesting question is whether the Ising type behavior is changed into the quasi-Heisenberg type at high pressure above QCEP, together with the topological change of Fermi surface. A conservative view is to assume that the Ising character is preserved through QCEP and thus the plateau observed above P_{QCEP} cannot be associated with a nematic phase. Key experiments will be magnetization, Hall effect, and thermopower measurements under pressure at high fields. If UCoAl will be a weak ferromagnet, as it is the case

for $\text{URhGe}^{21–23)}$ and $\text{UCoGe}^{25,60)}$ one can expect that transverse field perpendicular to M_0 will have strong effect on the ferromagnetic instability. Here excellent agreement is found with the view that tilting the field-angle only modifies the Zeeman energy.

5. Summary

We grew single crystals of UCoAl and performed resistivity and magnetostriction measurements under pressure up to 2.4 GPa and at high fields up to 16 T. The metamagnetic transition at H_m changes from the 1st order at low temperature to the crossover at high temperature. The critical temperature T_0 is determined by the field sweep of resistivity and magnetostriction measurements. With increasing pressure, H_m monotonously increases, while T_0 decreases and is suppressed at the quantum critical endpoint (QCEP). The field dependence of the effective mass detected by the resistivity A coefficient reveals the acute enhancement at QCEP at H_m . Further increasing pressure, H_m increases continuously as the crossover, which was detected both by resistivity and magnetostriction. The resistivity measurements exhibit another new anomaly at higher field H^* than H_m at pressures above P_{QCEP} . Our experiments show that UCoAl will be a key example of field-induced state built from ferromagnetic fluctuations. Its rather low values of $P_{\text{QCEP}} \sim 1.5\text{ GPa}$ and $H_{\text{QCEP}} \sim 7\text{ T}$ will allow one to perform a large variety microscopic and macroscopic experiments, which can provide definitive conclusions on the properties of QCEP and in the plateau regime detected at $P > P_{\text{QCEP}}$.

Acknowledgements

We thank H. Harima, L. Malone and A. P. Mackenzie for useful discussions. This work was supported by ERC starting grant (NewHeavyFermion), French ANR project (CORMAT, SINUS, DELICE).

- 1) J. Flouquet: *Progress in Low Temperature Physics*, ed. W. P. Halperin (Elsevier, Amsterdam, 2006) p. 139.
- 2) J. Flouquet, D. Aoki, W. Knafo, G. Knebel, T. D. Matsuda, S. Raymond, C. Proust, C. Paulsen and P. Haen: *J. Low Temp. Phys.* **161** (2010) 83.
- 3) R. A. Fisher, C. Marcenat, N. E. Phillips, P. Haen, F. Lapiere, P. Lejay, J. Flouquet and J. Voiron: *J. Low Temp. Phys.* **84** (1-2) (1991) 49.
- 4) D. Aoki, C. Paulsen, T. D. Matsuda, L. Malone, G. Knebel, P. Haen, P. Lejay, R. Settai, Y. Ōnuki and J. Flouquet: *J. Phys. Soc. Jpn.* **80** (2011) 053702.
- 5) V. Taufour, D. Aoki, G. Knebel and J. Flouquet: *Phys. Rev. Lett.* **105** (21) (2010) 217201.
- 6) H. Kotegawa, V. Taufour, D. Aoki, G. Knebel and J. Flouquet: to be published in *J. Phys. Soc. Jpn.*
- 7) M. Uhlarz, C. Pfeleiderer and S. M. Hayden: *Phys. Rev. Lett.* **93** (25) (2004) 256404.
- 8) S. A. Grigera, R. S. Perry, A. J. Schofield, M. Chiao, S. R. Julian, G. G. Lonzarich, S. I. Ikeda, Y. Maeno, A. J. Millis and A. P. Mackenzie: *Science* **294** (2001) 329.
- 9) S. S. Saxena, P. Agarwal, K. Ahilan, F. M. Grosche, R. K. W. Haselwimmer, M. J. Steiner, E. Pugh, I. R. Walker, S. R. Julian, P. Monthoux, G. G. Lonzarich, A. Huxley, I. Sheikin, D. Braithwaite and J. Flouquet: *Nature* **406** (2000) 587.
- 10) I. Sheikin, A. Huxley, D. Braithwaite, J. P. Brison, S. Watanabe, K. Miyake and J. Flouquet: *Phys. Rev. B* **64** (2001) 220503.
- 11) A. V. Andreev, R. Z. Levitin, Y. F. Popov and R. Y. Yumaguzhin: *Sov. Phys. Solid State* **27** (1985) 1145.
- 12) A. V. Andreev, K. Koyama, N. V. Mushnikov, V. Sechovský, Y. Shiokawa, I. Satoh and K. Watanabe: *J. Alloys Comp.* **441** (2007) 33.

- 13) Y. Ishii, M. Kosaka, Y. Uwatoko, A. V. Andreev and V. Sechovský: *Physica B* **334** (2003) 160.
- 14) N. V. Mushnikov, T. Goto, K. Kamishima, H. Yamada, A. V. Andreev, Y. Shiokawa, A. Iwao and V. Sechovský: *Phys. Rev. B* **90** (1999) 6877.
- 15) K. Koyama-Nakazawa, M. Koeda, M. Hedo and Y. Uwatoko: *Rev. Sci. Instr.* **78** (2007) 066109.
- 16) K. Yokogawa, K. MURATA, H. Yoshino and S. Aoyama: *Jpn. J. Appl. Phys.* **46** (2007) 3636.
- 17) L. Havela, A. V. Andreev, V. Sechovský, I. K. Kozlovskaya, K. Prokeš, P. Javorský, M. I. Bartashevich, T. Goto and K. Kamishima: *Physica B* **230-232** (1997) 98.
- 18) T. D. Matsuda, Y. Aoki, H. Sugawara, H. Sato, A. V. Andreev and V. Sechovsky: *J. Phys. Soc. Jpn.* **68** (1999) 3922.
- 19) N. V. Mushnikov, A. V. Andreev, T. Goto and V. Sechovský: *Philos. Mag. B* **81** (2001) 569.
- 20) D. Aoki, A. Huxley, E. Ressouche, D. Braithwaite, J. Flouquet, J.-P. Brison, E. Lhotel and C. Paulsen: *Nature* **413** (2001) 613.
- 21) F. Lévy, I. Sheikin and A. Huxley: *Nature Physics* **3** (2007) 460.
- 22) A. Miyake, D. Aoki and J. Flouquet: *J. Phys. Soc. Jpn.* **78** (2009) 063703.
- 23) D. Aoki, T. D. Matsuda, F. Hardy, C. Meingast, V. Taufour, E. Hassinger, I. Sheikin, C. Paulsen, G. Knebel, H. Kotegawa and J. Flouquet: *J. Phys. Soc. Jpn.* **80** (2011) SA008.
- 24) N. T. Huy, A. Gasparini, D. E. de Nijs, Y. Huang, J. C. P. Klaasse, T. Gortemulder, A. de Visser, A. Hamann, T. Görlach and H. v. Löhneysen: *Phys. Rev. Lett.* **99** (2007) 067006.
- 25) D. Aoki, T. D. Matsuda, V. Taufour, E. Hassinger, G. Knebel and J. Flouquet: *J. Phys. Soc. Jpn.* **78** (2009) 113709.
- 26) Y. Ihara, T. Hattori, K. Ishida, Y. Nakai, E. Osaki, K. Deguchi, N. K. Sato and I. Satoh: *Phys. Rev. Lett.* **105** (2010) 206403.
- 27) S. A. Grigera, R. A. Borzi, A. P. Mackenzie, S. R. Julian, R. S. Perry and Y. Maeno: *Phys. Rev. B* **67** (2003) 214427.
- 28) F. Honda, T. Kagayama, G. Oomi, L. Havela, V. Sechovský and A. Andreev: *Physica B* **284-288** (2000) 1299.
- 29) K. Miyake and O. Narikiyo: *J. Phys. Soc. Jpn.* **71** (3) (2002) 867.
- 30) D. Belitz, T. R. Kirkpatrick and Jörg Rollbühler: *Phys. Rev. Lett.* **94** (24) (2005) 247205.
- 31) V. Mineev: *C. R. Physique* **12**, 567 (2011).
- 32) K. G. Sandeman, G. G. Lonzarich and A. J. Schofield: *Phys. Rev. Lett.* **90** (16) (2003) 167005.
- 33) B. Binz and M. Sgrist: *Europhys. Lett.* **65** (2004) 816.
- 34) M. Shimizu: *Proc. Phys. Soc.* **84** (1964) 397.
- 35) A. J. Millis, A. J. Schofield, G. G. Lonzarich and S. A. Grigera: *Phys. Rev. Lett.* **88** (2002) 217204.
- 36) H. Yamada: *Phys. Rev. B* **47** (17) (1993) 11211.
- 37) Y. Yamaji, T. Misawa and M. Imada: *J. Phys. Soc. Jpn.* **76** (2007) 063702.
- 38) C. Pfleiderer and A. D. Huxley: *Phys. Rev. Lett.* **89** (2002) 147005.
- 39) K. Satoh, S. W. Yun, I. Umehara, Y. Ōnuki, S. Uji, T. Shimizu and H. Aoki: *J. Phys. Soc. Jpn.* **61** (1992) 1827.
- 40) T. Terashima, T. Matsumoto, C. Terakura, S. Uji, N. Kimura, M. Endo, T. Komatsubara and H. Aoki: *Phys. Rev. Lett.* **87** (16) (2001) 166401.
- 41) R. Settai, M. Nakashima, S. Araki, Y. Haga, T. C. Kobayashi, N. Tateiwa, H. Yamagami and Y. Ōnuki: *J. Phys.: Condens. Matter* **14** (2002) L29.
- 42) Y. Haga, M. Nakashima, R. Settai, S. Ikeda, T. Okubo, S. Araki, T. C. K. N. Tateiwa and Y. Ōnuki: *J. Phys.: Condens. Matter* **14** (2002) L125.
- 43) T. Terashima, T. Matsumoto, C. Terakura, S. Uji, N. Kimura, M. Endo, T. Komatsubara, H. Aoki and K. Maezawa: *Phys. Rev. B* **65** (2002) 174501.
- 44) R. Settai, M. Nakashima, H. Shishido, Y. Haga, H. Yamagami and Y. Ōnuki: *Acta Physica Polonica B* **34** (2003) 725.
- 45) H. Yamagami and A. Hasegawa: *Physica B* **186-188** (1993) 182.
- 46) A. B. Shick and W. E. Pickett: *Phys. Rev. Lett.* **86** (2) (2001) 300.
- 47) O. Eriksson, B. Johansson and M. S. S. Brooks: *J. Phys.: Condens. Matter* **1** (1989) 4005.
- 48) K. Betsuyaku and H. Harima: *Physica B* **281-282** (2000) 778.
- 49) T. D. Matsuda, H. Sugawara, Y. Aoki, H. Sato, A. V. Andreev, Y. Shiokawa, V. Sechovsky and L. Havela: *Phys. Rev. B* **62** (2000) 13852.
- 50) N. Kimura, M. Endo, T. Isshiki, S. Minagawa, A. Ochiai, H. Aoki, T. Terashima, S. Uji, T. Matsumoto and G. G. Lonzarich: *Phys. Rev. Lett.* **92** (19) (2004) 197002.
- 51) S. Watanabe, A. Tsuruta, K. Miyake and J. Flouquet: *J. Phys. Soc. Jpn.* **78** (10) (2009) 104706.
- 52) H. Shishido, K. Hashimoto, T. Shibauchi, T. Sasaki, H. Oizumi, N. Kobayashi, T. Takamasu, K. Takehana, Y. Imanaka, T. D. Matsuda, Y. Haga, Y. Onuki and Y. Matsuda: *Phys. Rev. Lett.* **102** (15) (2009) 156403.
- 53) M. M. Altarawneh, N. Harrison, S. E. Sebastian, L. Balicas, P. H. Tobash, J. D. Thompson, F. Ronning and E. D. Bauer: *Phys. Rev. Lett.* **106** (14) (2011) 146403.
- 54) L. Malone, T. D. Matsuda, A. Antunes, G. Knebel, V. Taufour, D. Aoki, K. Behnia, C. Proust and J. Flouquet: *Phys. Rev. B* **83** (2011) 245117.
- 55) R. A. Borzi, S. A. Grigera, J. Farrell, R. S. Perry, S. J. S. Lister, S. L. Lee, D. A. Tennant, Y. Maeno and A. P. Mackenzie: *Science* **315** (2007) 214.
- 56) E. Fradkin, S. A. Kivelson, M. J. Lawler, J. P. Eisenstein and A. P. Mackenzie: *Annual Rev. Cond. Mat. Phys.* **1** (2010) 153.
- 57) C. Sekine, T. Sakakibara, H. Amitsuka and Y. M. Goto: *J. Phys. Soc. Jpn.* **61** (12) (1992) 4536.
- 58) M. Sato, Y. Koike, S. Katano, N. Metoki, H. Kadowaki and S. Kawarazaki: *J. Phys. Soc. Jpn.* **73** (12) (2004) 3418.
- 59) W. Wu, A. McCollam, S. A. Grigera, R. S. Perry, A. P. Mackenzie and S. R. Julian: *Phys. Rev. B* **83** (4) (2011) 045106.
- 60) D. Aoki and J. Flouquet: to be published in *J. Phys. Soc. Jpn.*